A new underground measurement of the $^{14}N(p,\gamma)^{15}O$ reaction at the Bellotti Ion Beam Facility

Alessandro Compagnucci

The $^{14}N(p,\gamma)^{15}O$ and the CNO cycle

- The CNO Cycle is the main source of energy generation in massive main-sequence stars, accounts for **~1% in the Sun.**
- The $^{14}N(p,\gamma)^{15}O$ is the **slowest reaction of the CNO**, controls its speed and energy production rate.

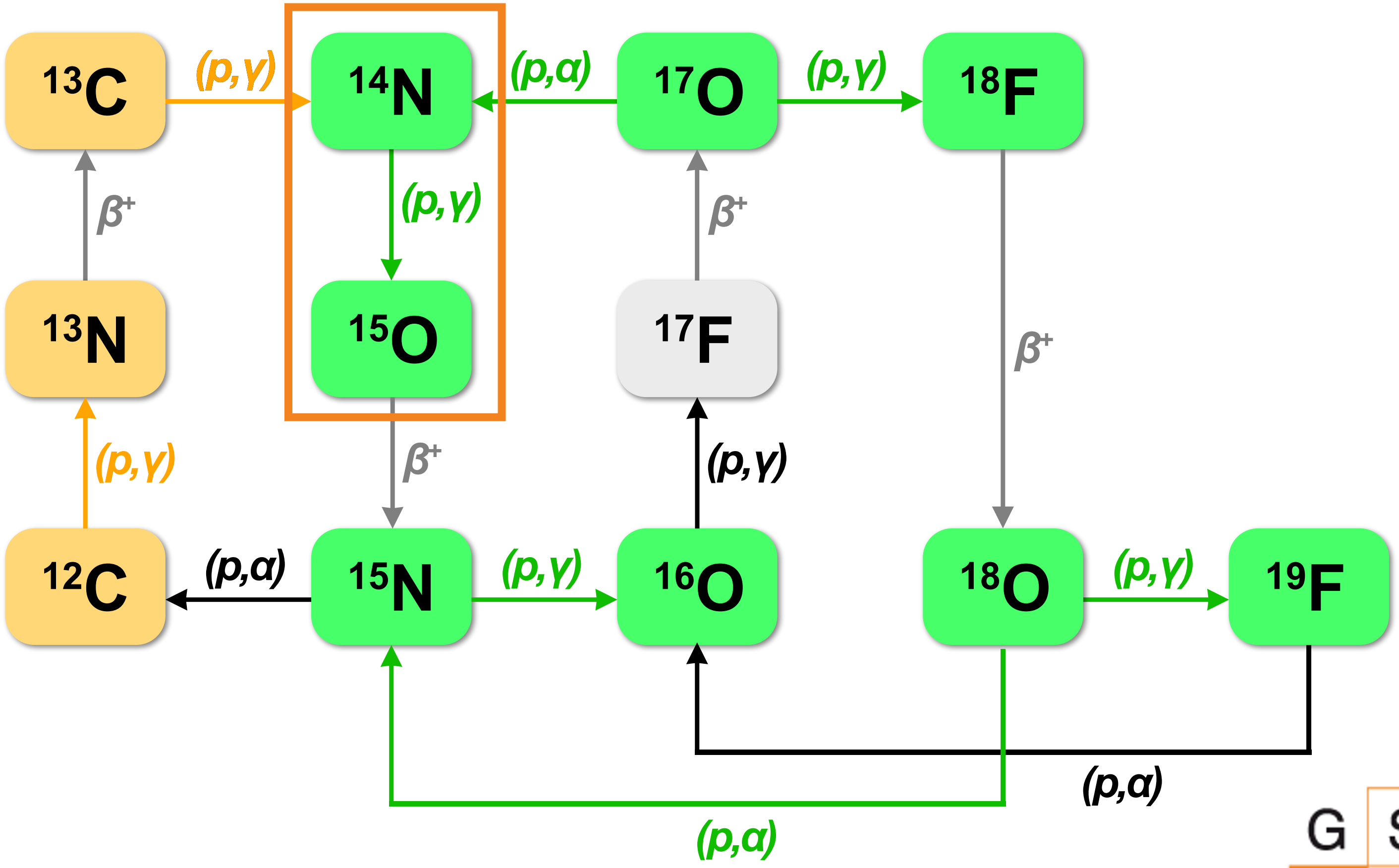

The $^{14}N(p,\gamma)^{15}O$ and the CNO cycle

- **Solar CNO neutrino flux** recently detected for the first time by Borexino (2020). → **Solar metallicity probe.**
- The result of Borexino disfavours "low metallicity" SSM prediction, **but large uncertainties** still remains. After CNO Flux itself, biggest contribution to the uncertainty budget from $^{14}N(p,\gamma)^{15}O$ cross section.

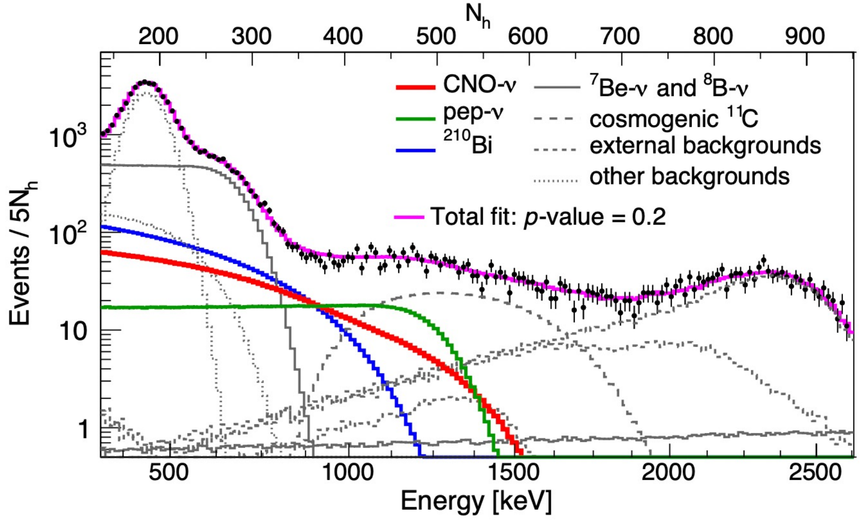

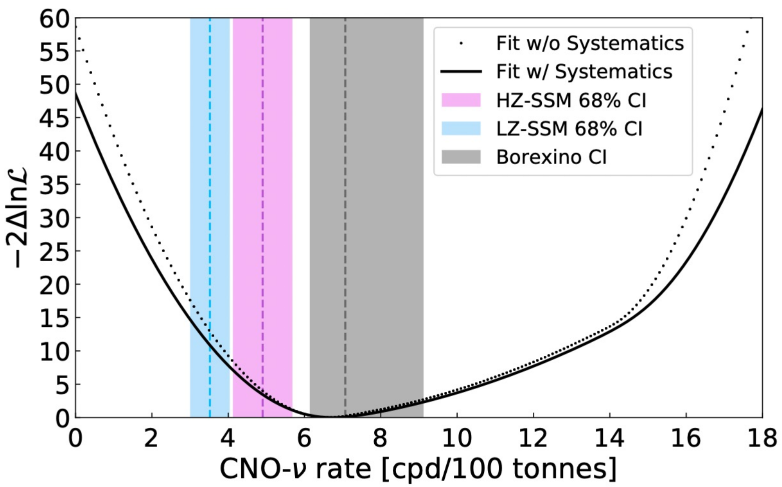

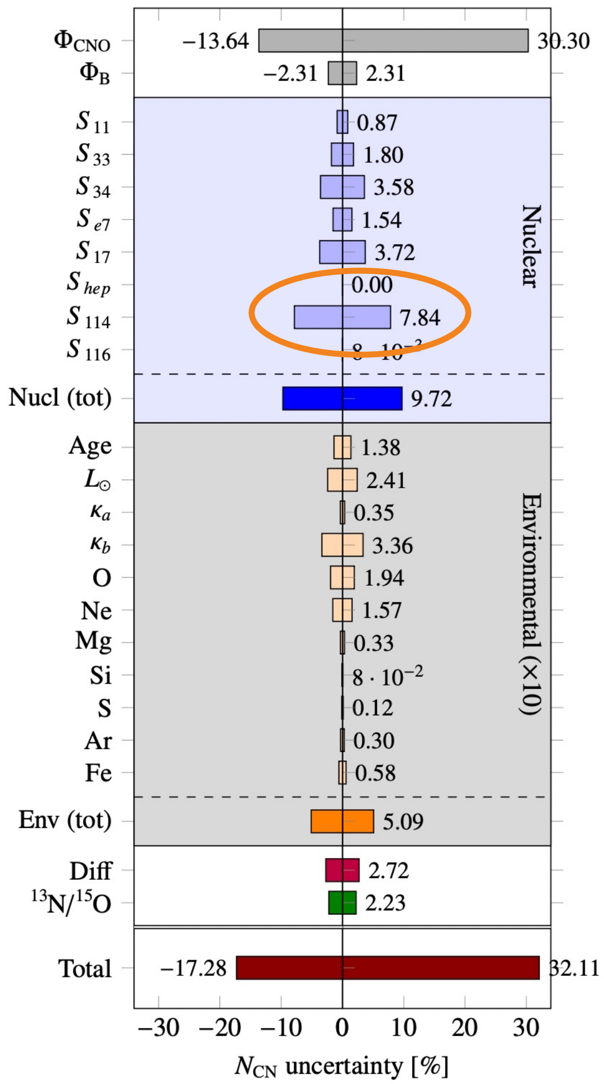

Appel, S. et al. (2022) PRL

Open issues with $^{14}N(p,\gamma)^{15}O$

- The transition to the **6.79 MeV** excited state of ^{15}O and to the **ground state** are fairly well know but effected to problems with their extrapolations at low energies

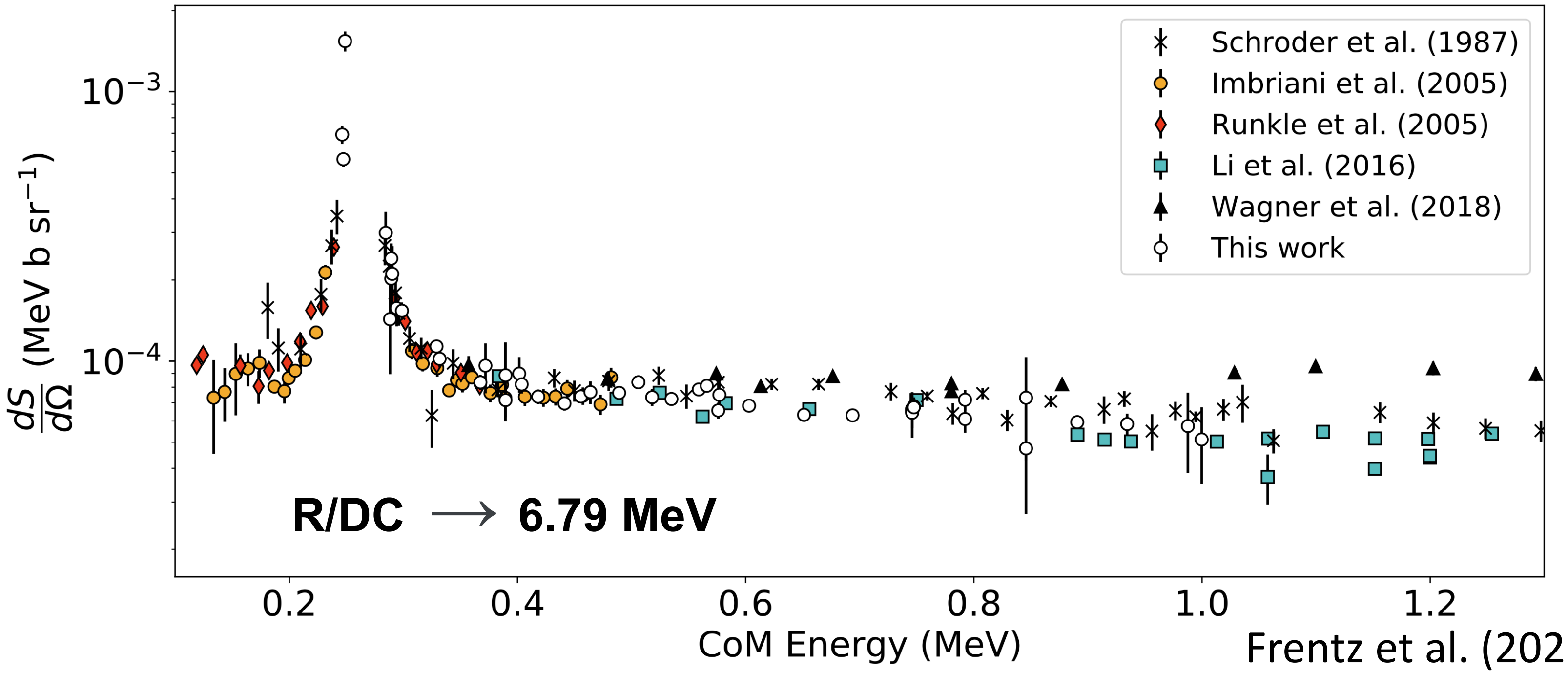

Frentz et al. (2022)

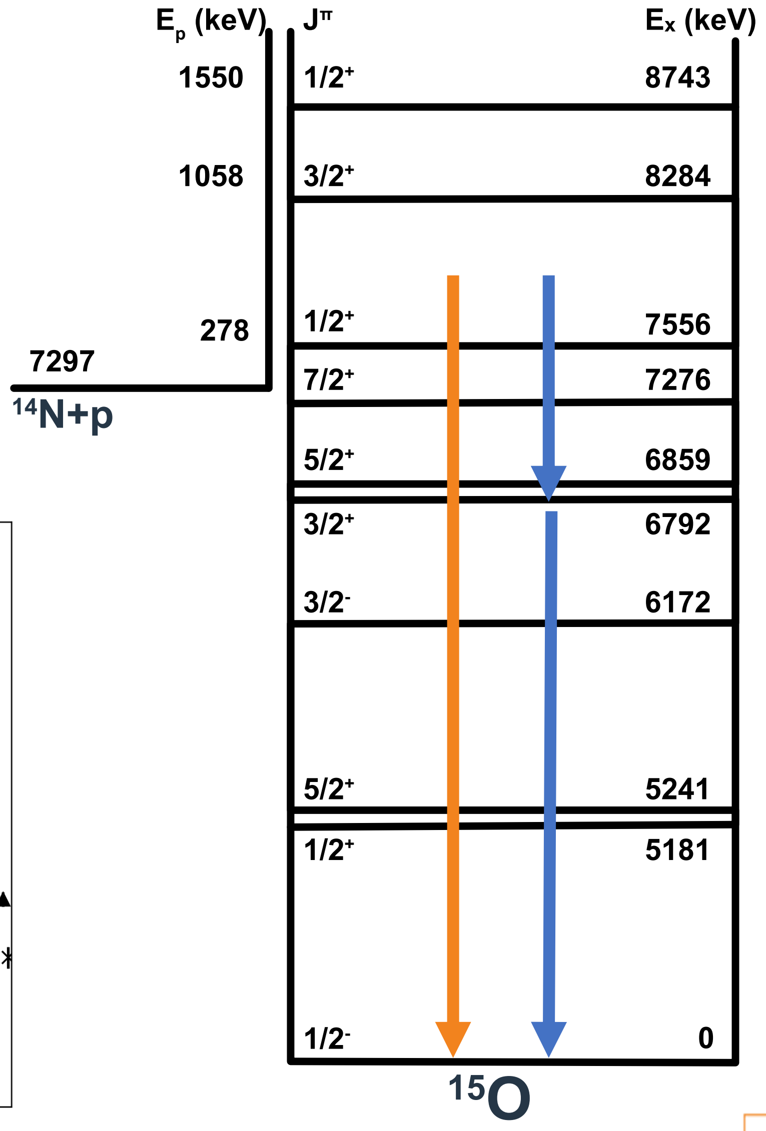

Level scheme for ^{15}O

Open issues with $^{14}N(p,\gamma)^{15}O$

- The transition to the **6.79 MeV** excited state of ^{15}O and to the **ground state** are fairly well know but effected to problems with their extrapolations at low energies

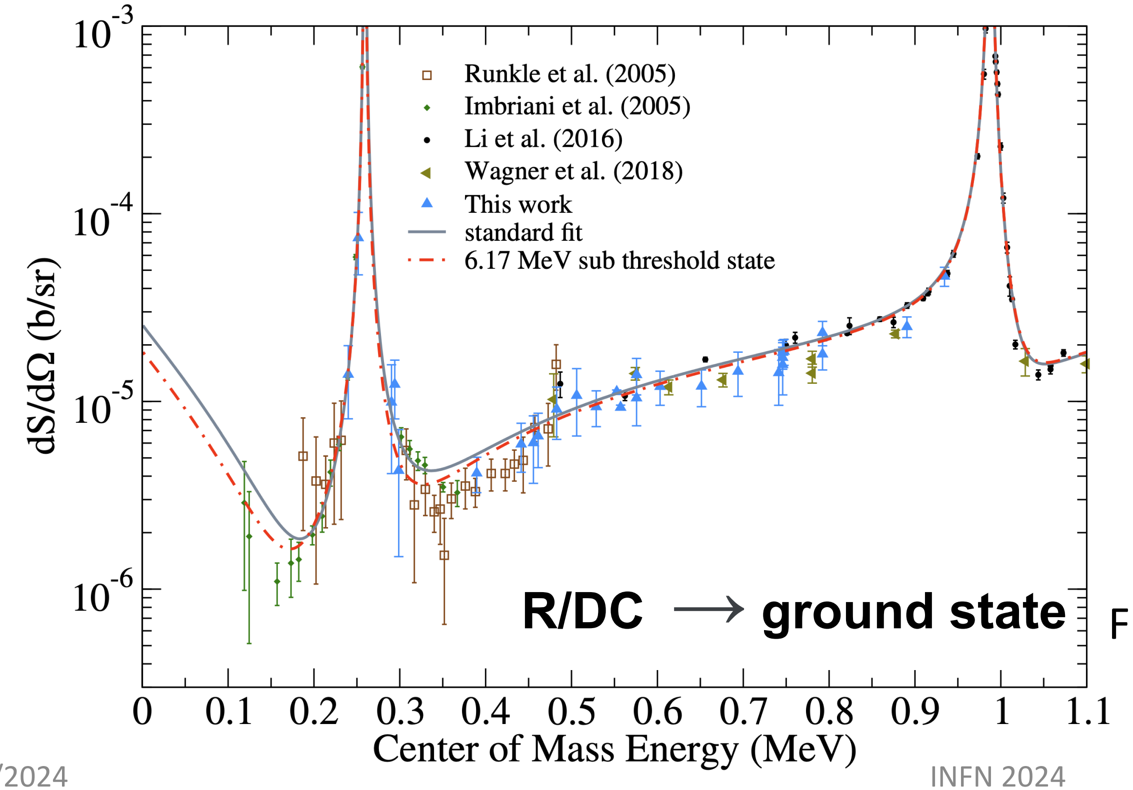

Frentz et al (2022)

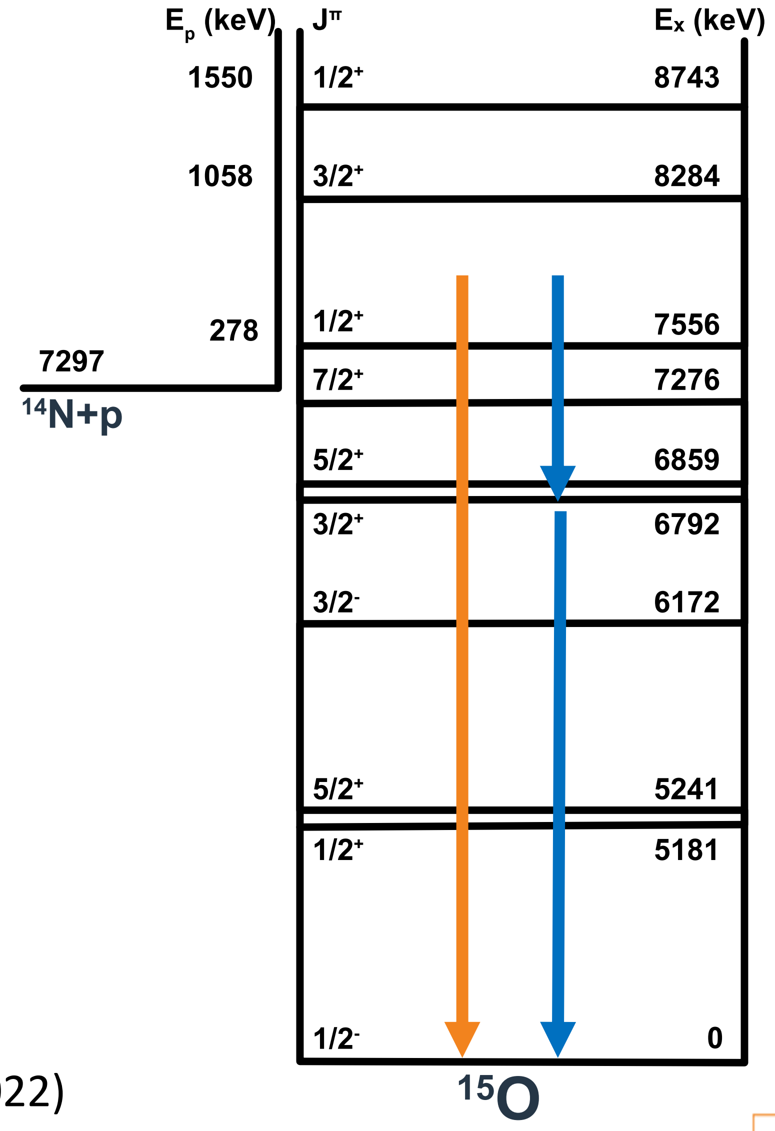

Level scheme for ^{15}O

Open issues with $^{14}N(p,\gamma)^{15}O$

- The transition to the **6.79 MeV** excited state of ^{15}O and to the **ground state** are fairly well know but effected to problems with their extrapolations at low energies

TABLE I. A summary of zero energy S factors for the $^{14}N(p,\gamma)^{15}O$ reaction.

Year	Reference	Astrophysical S factor $S(0)$ (keV b): R/DC → 0.00	R/DC → 6.792	R/DC → 6.172	Others[d]	Total
1987	Schröder *et al.* [9]	1.55 ± 0.34	1.41 ± 0.02	0.14 ± 0.05	0.1	3.20 ± 0.54
2001	Angulo *et al.*[a] [10]	$0.08^{+0.13}_{-0.06}$	1.63 ± 0.17	$0.06^{+0.01}_{-0.02}$	——	1.77 ± 0.20
2003	Mukhamedzhanov *et al.* [16]	0.15 ± 0.07	1.40 ± 0.20	0.133 ± 0.02	0.02	1.70 ± 0.22
2004	Formicola *et al.* [17]	0.25 ± 0.06	1.35 ± 0.05 (stat) ± 0.08 (sys)	$0.06^{+0.01}_{-0.02}$[b]	0.04	1.7 ± 0.1 (stat) ± 0.02 (sys)
2005	Imbriani *et al.* [11]	0.25 ± 0.06	1.21 ± 0.05	0.08 ± 0.03	0.07	1.61 ± 0.08
2005	Runkle *et al.* [15]	0.49 ± 0.08	1.15 ± 0.05	0.04 ± 0.01	——	1.68 ± 0.09
2005	Angulo *et al.* [18]	0.25 ± 0.08	1.35 ± 0.04	0.06 ± 0.02	0.04	1.70 ± 0.07 (stat) ± 0.10 (sys)
2006	Bemmerer *et al.* [13]	——	——	——	——	1.74 ± 0.14 (stat) ± 0.14 (sys)[c]
2008	Marta *et al.* [14]	0.20 ± 0.05	——	0.09 ± 0.07	——	1.57 ± 0.13
2010	Azuma *et al.* [19]	0.28	1.3	0.12	0.11	1.81
2011	Adelberger *et al.* [3]	0.27 ± 0.05	1.18 ± 0.05	0.13 ± 0.06	0.08	1.66 ± 0.08
2016	Li *et al.* [20]	0.42 ± 0.04 (stat) $^{+0.09}_{-0.19}$(sys)	1.29 ± 0.06 (stat) ± 0.06 (sys)	——	——	——
2018	Wagner *et al.* [21]	0.19 ± 0.01 (stat) ± 0.05 (sys)	1.24 ± 0.02 (stat) ± 0.11 (sys)	——	——	——
2022	This work	$0.33^{+0.16}_{-0.08}$	1.24 ± 0.09	0.12 ± 0.04	——	1.69 ± 0.13

[a] *R*-matrix analysis on available data, not a measurement.
[b] Adopted from Angulo and Descouvement [10].
[c] Measured S factor at 70 keV.

Frentz et al (2022)

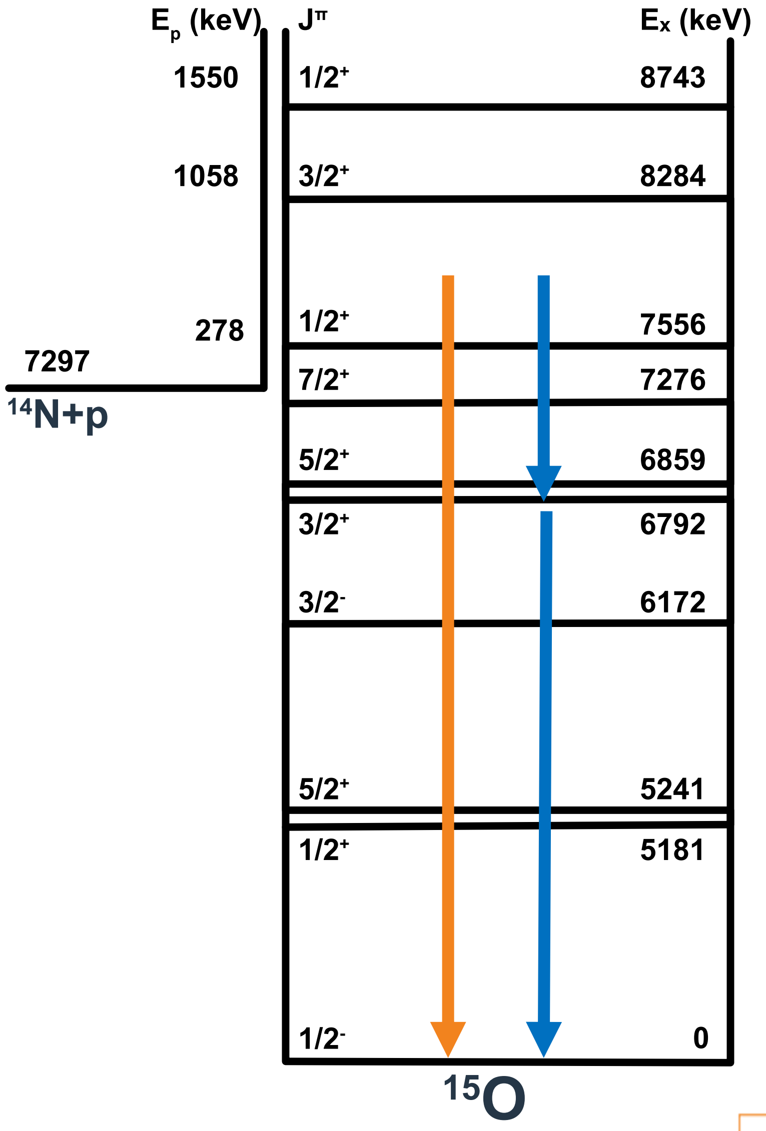

Level scheme for ^{15}O

Open issues with $^{14}N(p,\gamma)^{15}O$

- Lack of recent data for the other transitions
  R/DC → 6.17, 5.24, 5.18 ...

TABLE I. A summary of zero energy S factors for the $^{14}N(p,\gamma)^{15}O$ reaction.

		Astrophysical S factor $S(0)$ (keV b)				
Year	Reference	R/DC → 0.00	R/DC → 6.792	R/DC → 6.172	Others[d]	Total
1987	Schröder *et al.* [9]	1.55 ± 0.34	1.41 ± 0.02	0.14 ± 0.05	0.1	3.20 ± 0.54
2001	Angulo *et al.*[a] [10]	$0.08^{+0.13}_{-0.06}$	1.63 ± 0.17	$0.06^{+0.01}_{-0.02}$	−−	1.77 ± 0.20
2003	Mukhamedzhanov *et al.* [16]	0.15 ± 0.07	1.40 ± 0.20	0.133 ± 0.02	0.02	1.70 ± 0.22
2004	Formicola *et al.* [17]	0.25 ± 0.06	1.35 ± 0.05 (stat) ± 0.08 (sys)	$0.06^{+0.01}_{-0.02}$[b]	0.04	1.7 ± 0.1 (stat) ± 0.02 (sys)
2005	Imbriani *et al.* [11]	0.25 ± 0.06	1.21 ± 0.05	0.08 ± 0.03	0.07	1.61 ± 0.08
2005	Runkle *et al.* [15]	0.49 ± 0.08	1.15 ± 0.05	0.04 ± 0.01	−−	1.68 ± 0.09
2005	Angulo *et al.* [18]	0.25 ± 0.08	1.35 ± 0.04	0.06 ± 0.02	0.04	1.70 ± 0.07 (stat) ± 0.10 (sys)
2006	Bemmerer *et al.* [13]	−−	−−	−−	−−	1.74 ± 0.14 (stat) ± 0.14 (sys)[c]
2008	Marta *et al.* [14]	0.20 ± 0.05	−−	0.09 ± 0.07	−−	1.57 ± 0.13
2010	Azuma *et al.* [19]	0.28	1.3	0.12	0.11	1.81
2011	Adelberger *et al.* [3]	0.27 ± 0.05	1.18 ± 0.05	0.13 ± 0.06	0.08	1.66 ± 0.08
2016	Li *et al.* [20]	0.42 ± 0.04 (stat) $^{+0.09}_{-0.19}$(sys)	1.29 ± 0.06 (stat) ± 0.06 (sys)	−−	−−	−−
2018	Wagner *et al.* [21]	0.19 ± 0.01 (stat) ± 0.05 (sys)	1.24 ± 0.02 (stat) ± 0.11 (sys)	−−	−−	−−
2022	This work	$0.33^{+0.16}_{-0.08}$	1.24 ± 0.09	0.12 ± 0.04	−−	1.69 ± 0.13

[a] R-matrix analysis on available data, not a measurement.
[b] Adopted from Angulo and Descouvement [10].
[c] Measured S factor at 70 keV.

Frentz et al (2022)

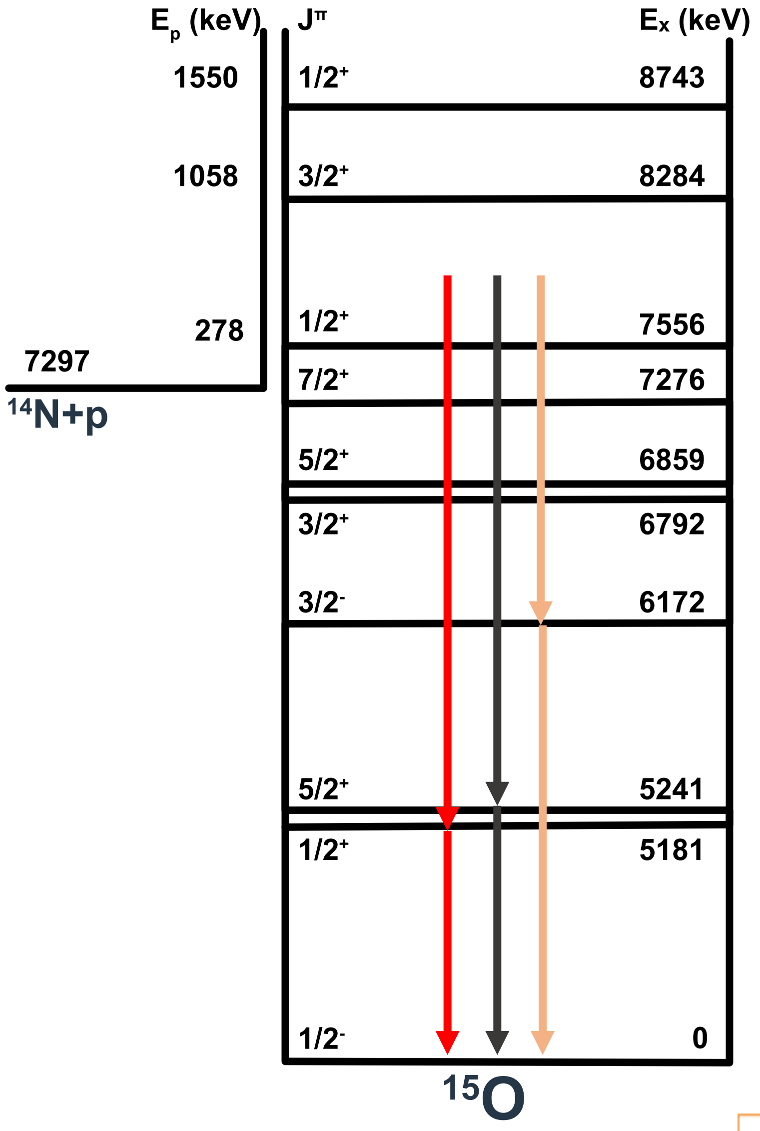

Level scheme for ^{15}O

Underground Nuclear Astrophysics at LUNA

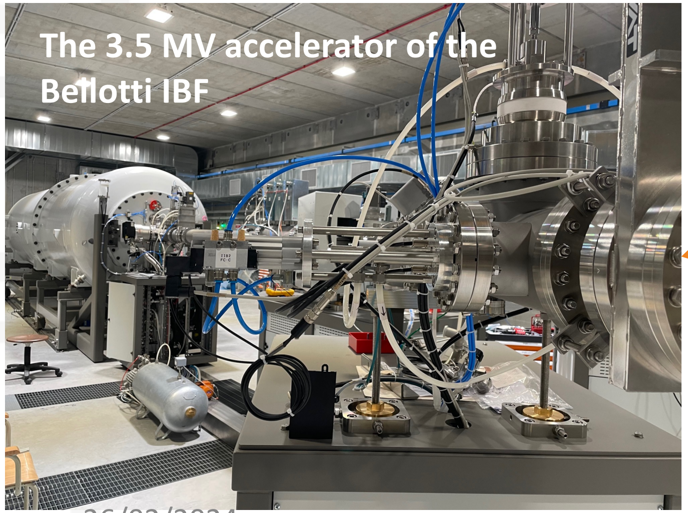

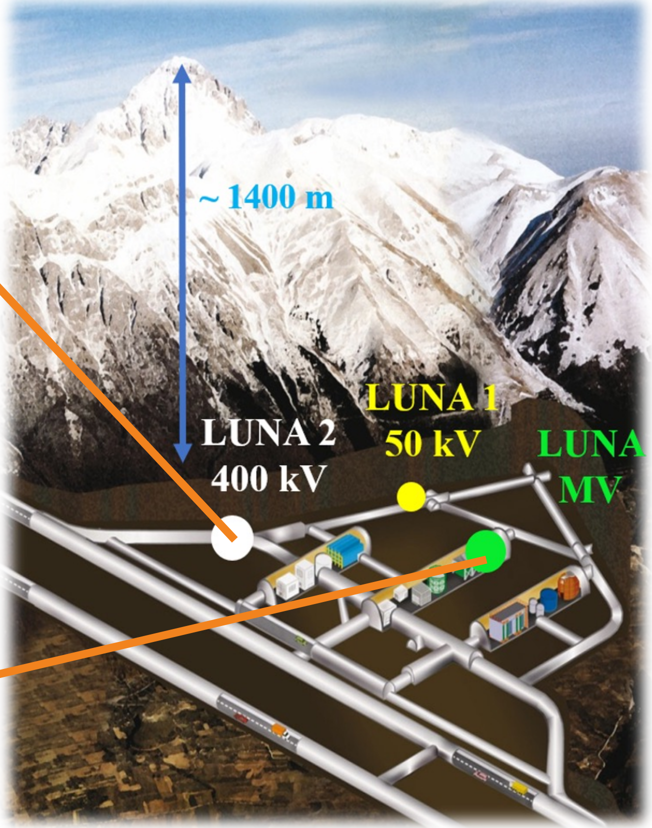

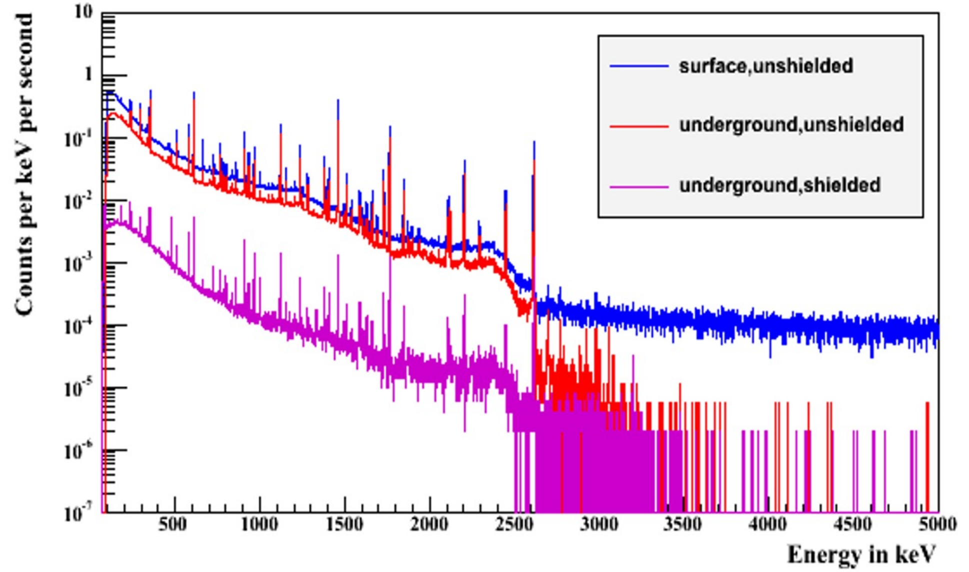

The Bellotti Ion Beam Facility of LNGS

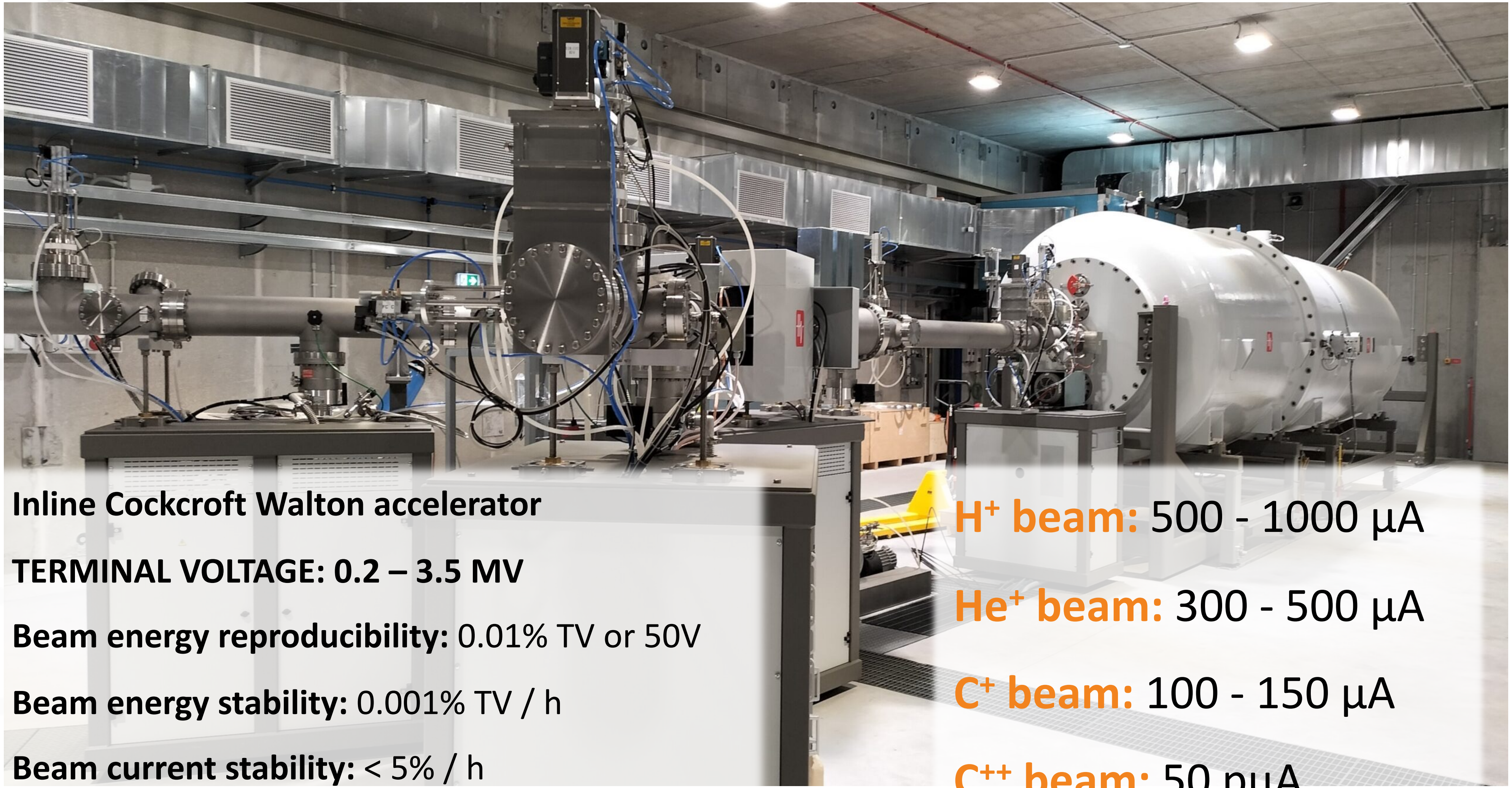

Inline Cockcroft Walton accelerator

TERMINAL VOLTAGE: 0.2 – 3.5 MV

Beam energy reproducibility: 0.01% TV or 50V

Beam energy stability: 0.001% TV / h

Beam current stability: < 5% / h

H^+ beam: 500 - 1000 μA

He^+ beam: 300 - 500 μA

C^+ beam: 100 - 150 μA

C^{++} beam: 50 pμA

The $^{14}N(p,\gamma)^{15}O$ measurement at the Bellotti IBF

- Low background measurement over a **wide-energy range**, in order to address the existing issues in the extrapolations
- **Angular distribution**
- Measuring **weaker transitions**
- Pilot LUNA project at the new facility
  → Verifing the **performance of the accelerator**
  → **Energy calibration** campaign ancillary to the measurements

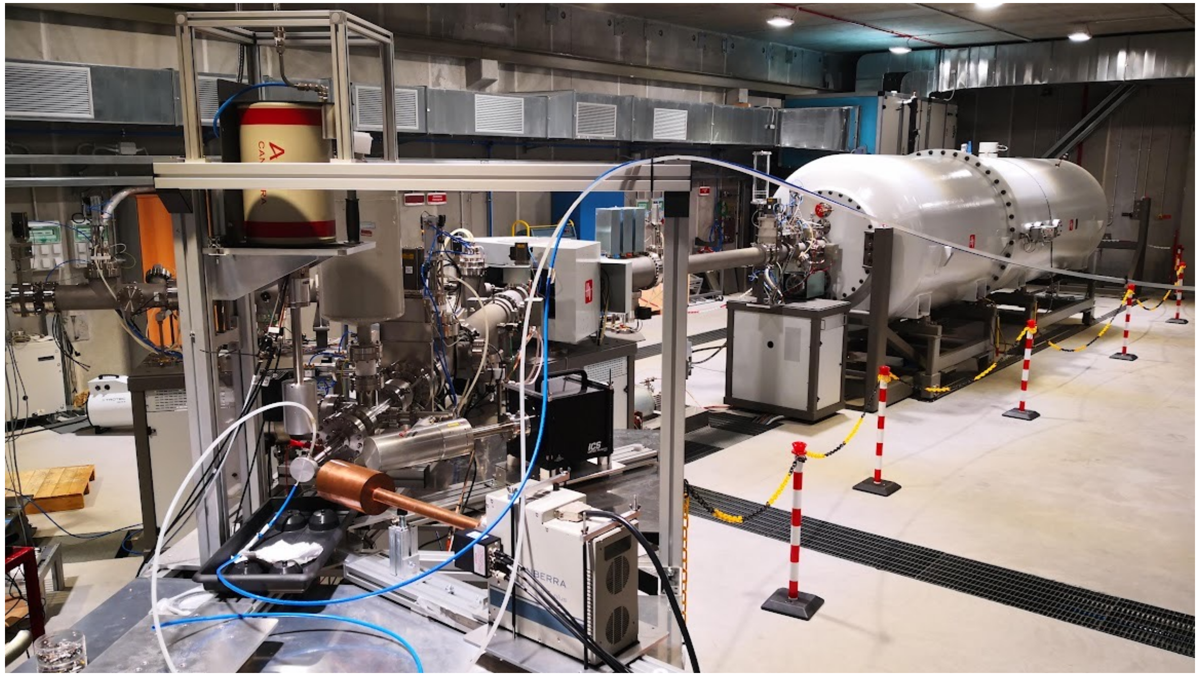

The $^{14}N(p,\gamma)^{15}O$ measurement at the Bellotti IBF

- Two phases:
  - Single HPGe detector in close geometry. **Excitation function**. (**completed, June 2023**)
  - Three HPGe detectors, **angular distribution** measurement. (**Started in October 2023**).

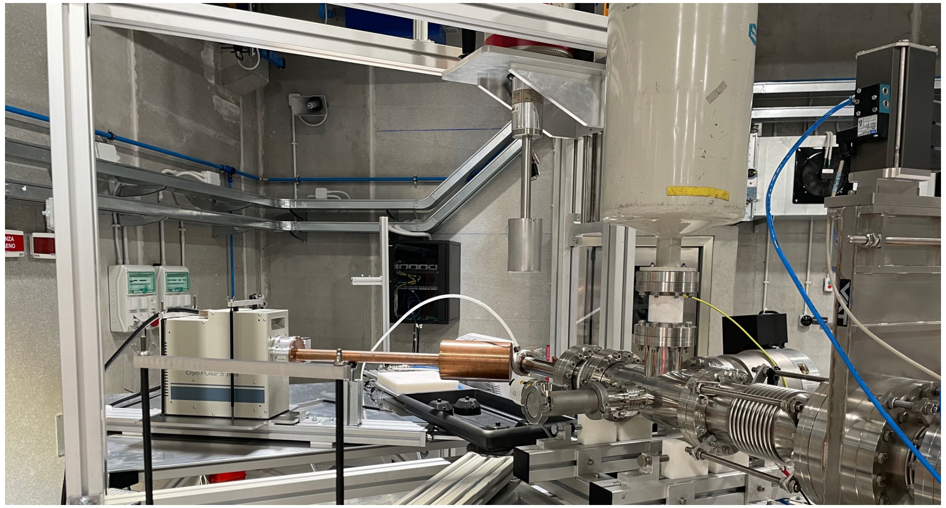

Solid Targets

- **Sputtered TaN targets**: Produced at LNL. Enriched (99.95%) nitrogen gas. Tested for stability up to 40+ C. Characterization via RBS and on-site using 278 keV 14N+p resonance scans.
- **Implanted targets**: Produced at IST, Lisbon. Tested for stability up to 15 C.

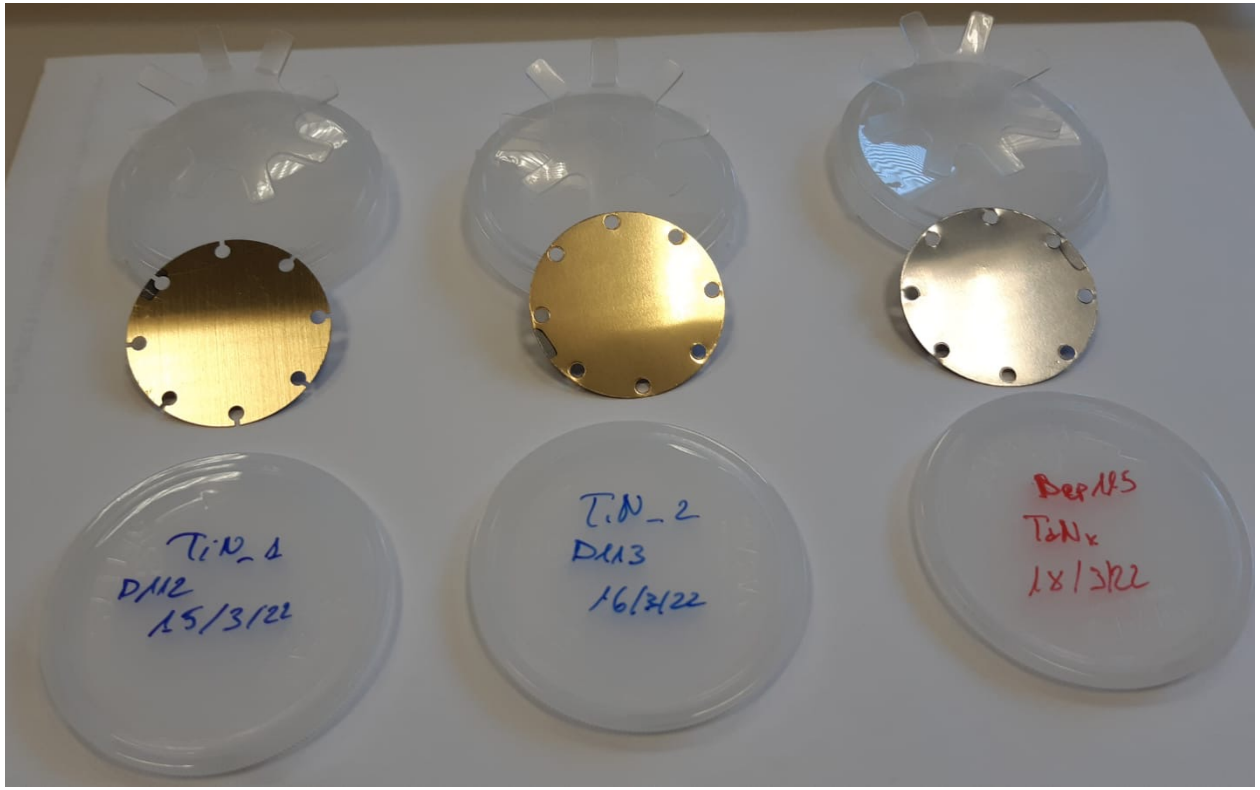

Solid Targets: Characterization of the contaminants

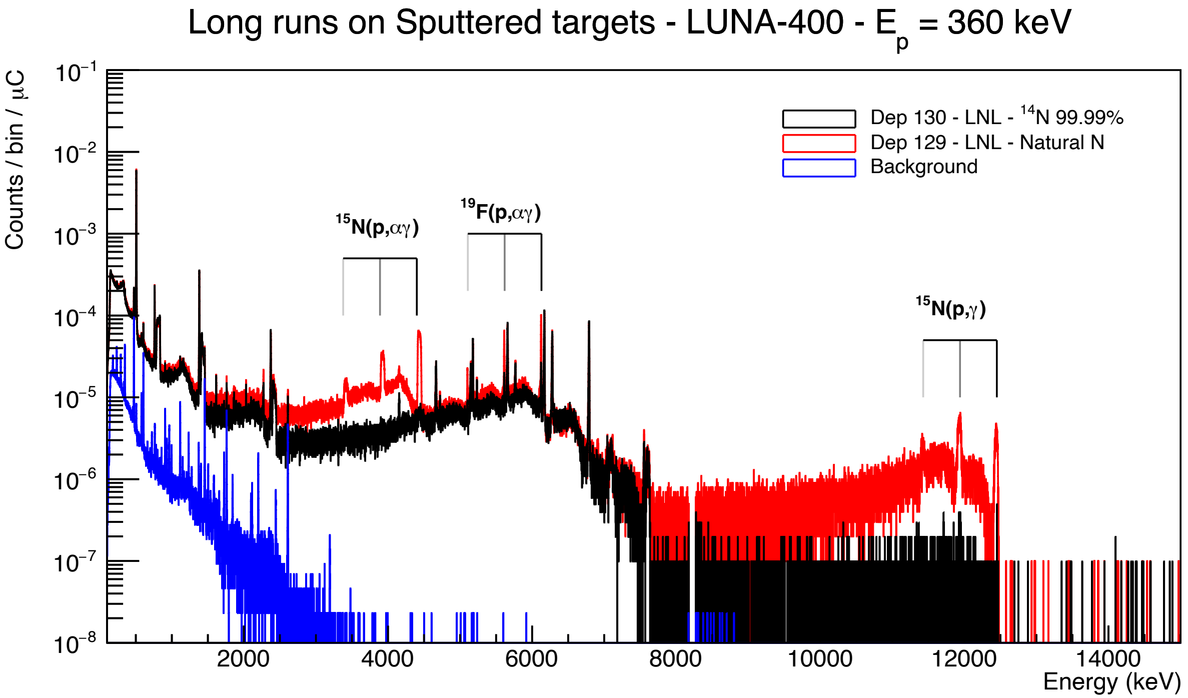

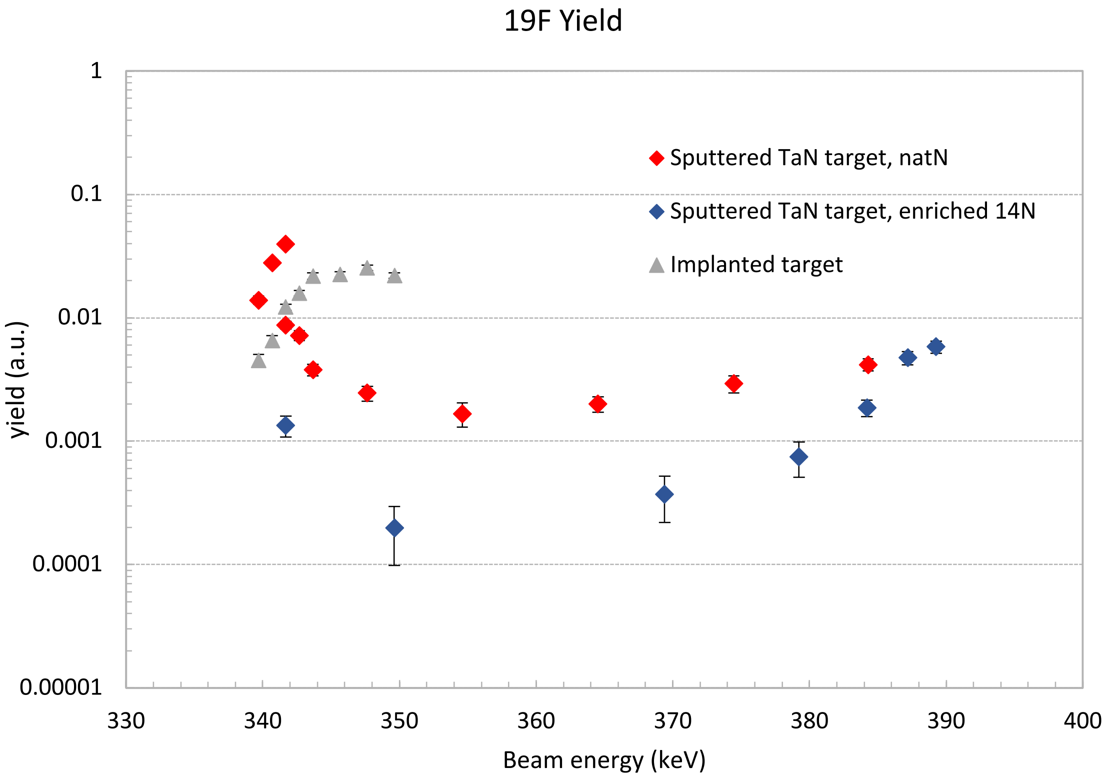

Significantly improved solid targets in terms of ^{15}N and ^{19}F contaminations!

Solid Targets: Stability monitoring

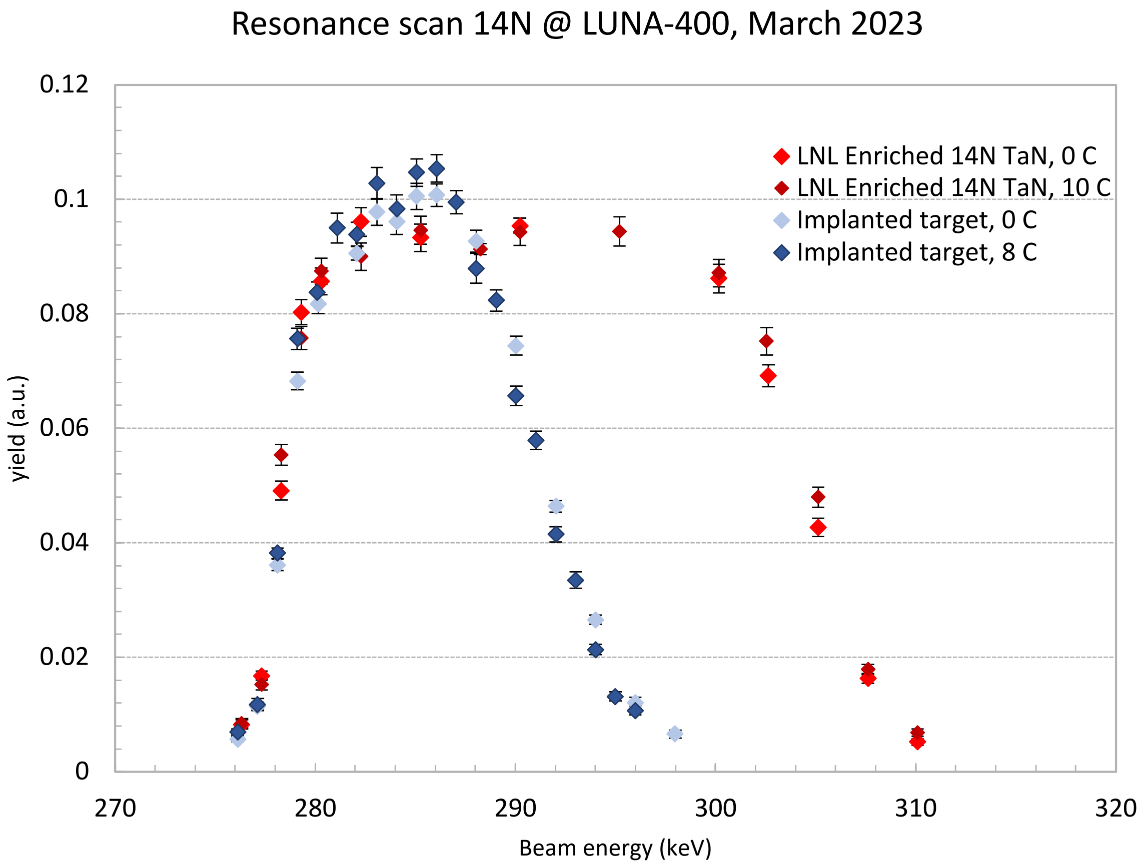

Resonance scan of 278 keV resonance for two TaN sputtered target with different thicknesses @ Bellotti IBF 3.5 MV accelerator

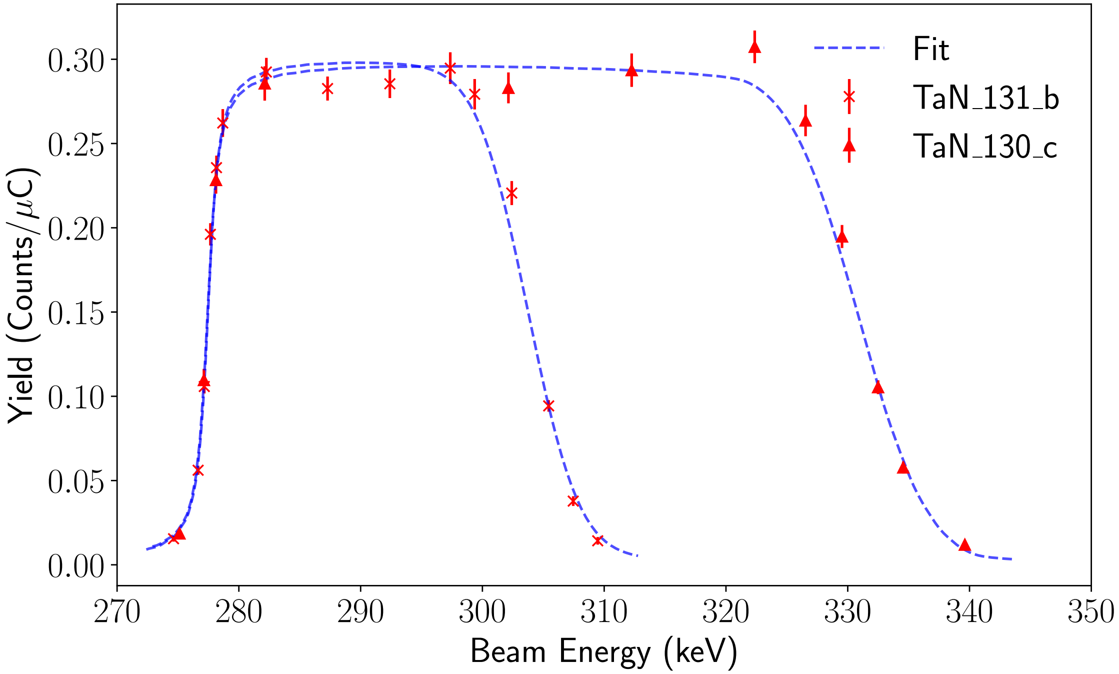

On site during the measurement

Efficiency characterization for the HPGe detector

- **Efficiency calibration** using ^{137}Cs, ^{60}Co and ^{14}N+p reaction
- Reaction data have been corrected for summing effects

$$\ln(\varepsilon_{fe}) = a + b\ln(E_\gamma) + c[\ln(E_\gamma)]^2\,,$$

$$\varepsilon_{fe}(d) = \frac{1 - e^{\frac{d+d_0}{1+\beta\sqrt{E_\gamma}}}}{(d+d_0)^2}\,.$$

$$Y_{gs} = R\left(b_{gs}\varepsilon_{fe}(E_{gs}) + \sum_i b_i\varepsilon_{fe}(E_i^{sec})\varepsilon_{fe}(E_i^{pri})\right)$$

$$Y_{i_{pri}} = Rb_i\varepsilon_{fe}(E_{i_{pri}})(1 - \varepsilon_{tot}(E_{i_{sec}}))\,,$$
$$Y_{i_{sec}} = Rb_i\varepsilon_{fe}(E_{i_{sec}})(1 - \varepsilon_{tot}(E_{i_{pri}}))\,,$$

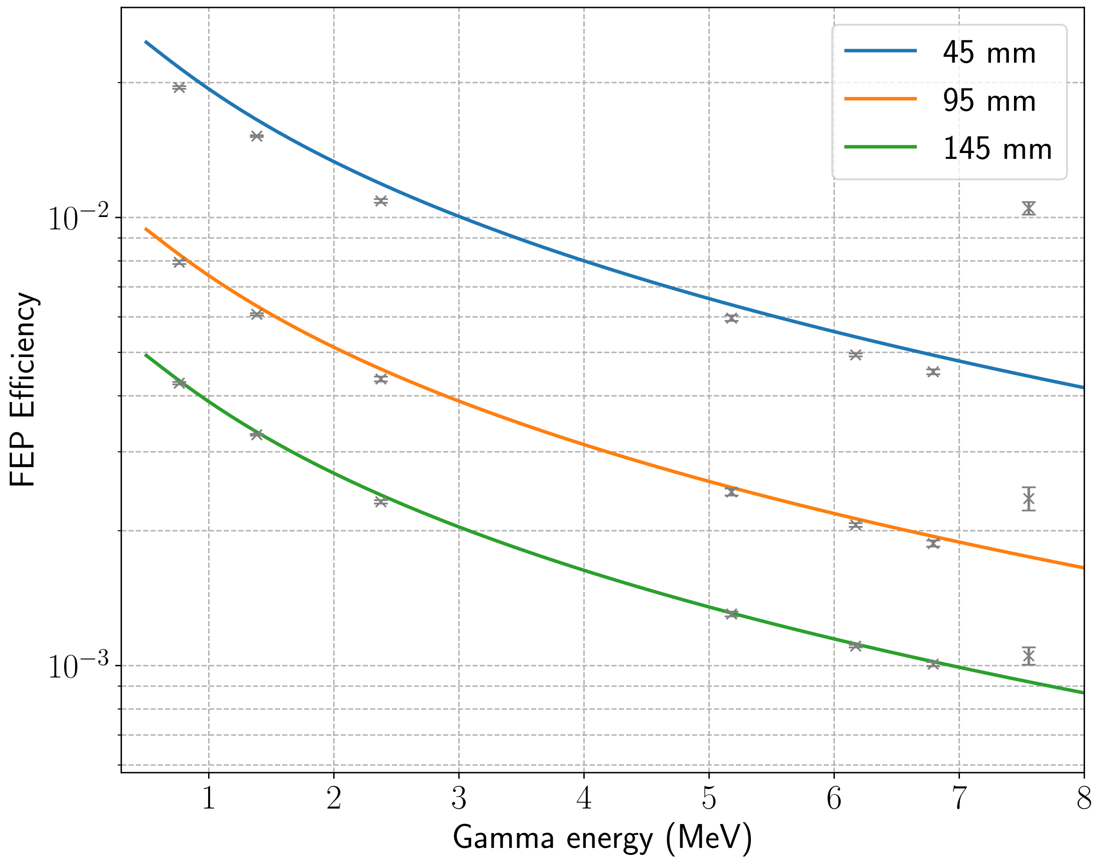

Preliminary results

- Data collected during the first beam time in **June 2023**
- Energy range covered: **0.25 - 1.3 MeV** in 50 keV steps
- one HPGe detector at 55° and 5 cm from the target.
- Three sputtered target and one implanted target
- Total charge collected: 38 C (up to 300 uA of current on target)

A typical gamma-ray spectrum

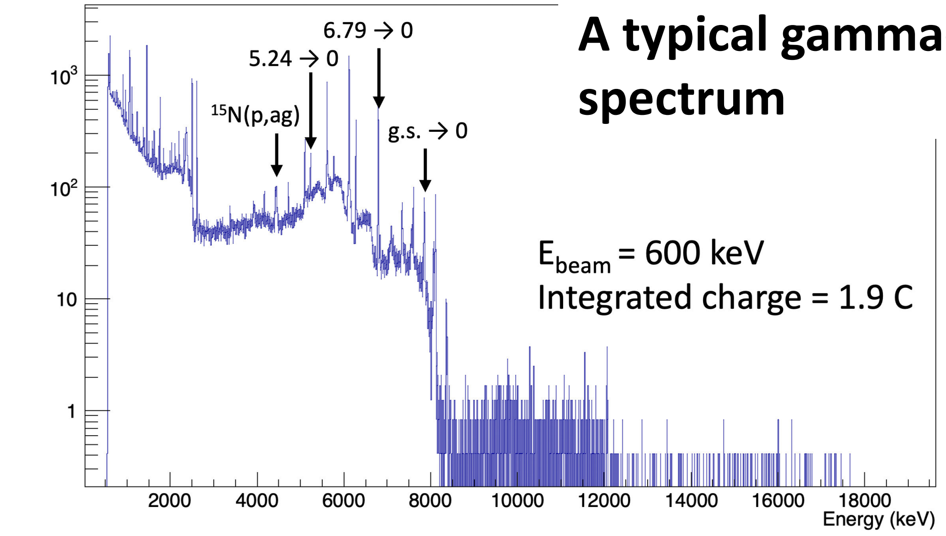

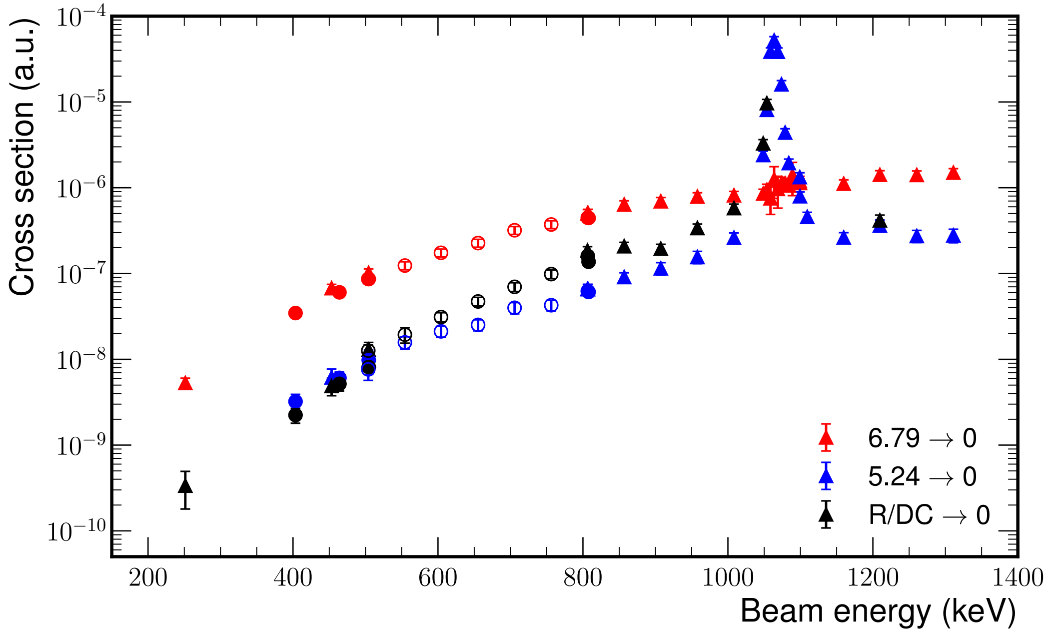

Conclusion

- Cross section data for the astrophysical key reaction $^{14}N(p,\gamma)^{15}O$ have been collected with one HPGe detector placed at 55° in the energy range **0.25 - 1.3 MeV**, for a total of 38 C of charge accumulated on 4 different targets.
- Most of the **weaker transitions**, many of them not observed by previous authors, are identifiable in the spectra and will be included in a comprehensive analysis of the dataset in progress.
- In a second phase of the experiment the **angular distributions** of the most important transitions of the reaction are being measured, most notably going below 600 keV where no literature data are available.
- These preliminary results showcase the strength of measuring this reaction in a deep-underground location taking advantage from the high current and excellent long term stability of the beam delivered by the 3.5 MV accelerator of the Bellotti IBF.

Thank you for your attention!

The LUNA collaboration

LUNA

luna.lngs.infn.it

GSSI